

PACS numbers: 42.55.Px; 42.60.Da; 32.80.Pj
DOI: 10.1070/QE2004v034n04ABEH002678

Tunable frequency-stabilised laser for studying the cooling dynamics of Rb atoms in a magnetooptical trap

A.V. Yarovitskii, O.N. Prudnikov, V.V. Vasil'ev, V.L. Velichansky, O.A. Razin, I.V. Sherstov, A.V. Taichenachev, V.I. Yudin

***Abstract*. A system is developed which allows one to stabilise the diode laser frequency at any point in the vicinity of the cyclic D_2-line transition in Rb in the interval from +40 to −150 MHz and to switch the laser frequency within this interval for ~ 1 ms. A method is proposed and realised for increasing the contrast of the reference sub-Doppler resonance observed in circularly polarised fields. The ultimate contrast of the resonance is estimated. This system can be used to study the anomalous light pressure force acting on atoms in an optical molasses. A magnetooptical trap for Rb atoms is described.**

Keywords: *frequency stabilisation, nonlinear sub-Doppler spectroscopy, laser cooling, diode laser*.

1. Introduction

The development of diode lasers resulted in the fabrication of many types of single-frequency tunable sources of coherent radiation. This was accompanied by the development of methods for laser frequency stabilisation [1], which are now used in various diode lasers. At present the frequency stabilisation was demonstrated for lasers of different types: uniformly pumped end-emitting lasers, non-uniformly pumped lasers with Bragg mirrors, vertical-cavity surface-emitting lasers (VCSELs) [2], and lasers with an external feedback. A diode laser with an external selective resonator and a broadband system of frequency stabilisation coupled to the resonance of a high-Q interferometer provides a high short-term stability and, using Ca atoms ($\lambda = 657$ nm), is employed in one of the primary frequency standards [3].

Many applications, in particular, laser cooling of atoms require simultaneously the high frequency stability and the possibility of precision frequency detuning from the atomic resonance. Magnetooptical traps (MOTs) are used to prepare ensembles of cooled atoms employed in atomic physics, spectroscopy, metrology, and physics of condensed media [4, 5]. Laser cooling is not only used as a tool in atomic physics and metrology but is also the object of investigation itself.

In particular, the possibility of the existence of a new frictional force acting on atoms in a laser field was predicted in Ref. [6]. It has the sub-Doppler mechanism of formation [7], which requires the degeneracy of the ground state over the projection of the angular momentum. The peculiarity of this force is its even dependence on the detuning of the cooling laser field frequency from the atomic resonance. Moreover, unlike the known radiation friction forces, the new force does not disappear in the case of an exact resonance.

Note that a standard MOT, which drastically suppresses the Doppler broadening, causes the broadening of atomic lines due to spatially inhomogeneous Zeeman and light shifts. The Zeeman shifts of levels are significant for the peripheral region of an atomic ensemble. A magnetic field in a purely viscous trap (molasses) can be made weak, but optical shifts will be perceptible when the atomic cloud size is comparable with a cooling beam diameter. Both Zeeman and optical shifts in a molasses can be suppressed with the help of a new force, which will alleviate studies in a stationary regime under homogeneous conditions for the entire atomic ensemble.

The new friction force was studied theoretically in Ref. [6] for atoms with the angular momentum $F = 1/2$ in the ground state in a one-dimensional field produced by counterpropagating elliptically polarised waves with identical amplitudes. Calculations performed for transitions with large ground-state angular momenta ($F = 1$, 2, etc.) [8] refined the details of formation of a new force related to the Zeeman coherence in the ground state. The prediction of the appearance of a new force remained invariable, so that a search for this force can be performed in Li, Na, K, and Rb isotopes.

In Ref. [6], the saturation of a transition was assumed weak (the Rabi frequency of laser fields is lower than the natural width of the transition: $\Omega \ll \gamma$) and a magnetic field was zero. It was shown in this paper that a new force appears if the polarisation ellipses of counterpropagating fields are identical, the directions of polarisation rotation are opposite, and the angle θ between the major semiaxes of ellipses lies between 0 and 45°. In the case of weak saturation, the Zeeman splitting should be much smaller than the optical shift: $\omega_H \ll \Omega^2/(\delta^2 + \gamma^2/4)^{1/2}$. This means

A.V. Yarovitskii, V.V. Vasil'ev, V.L. Velichansky, O.A. Razin, I.V. Sherstov P.N. Lebedev Physics Institute, Russian Academy of Sciences, Leninsky prosp. 53, 119991 Moscow, Russia;
O.N. Prudnikov Novosibirsk State University, ul. Pirogova 2, 630090 Novosibirsk, Russia;
A.V. Taichenachev, V.I. Yudin Institute of Laser Physics, Siberian Branch, Russian Academy of Sciences, prosp. Lavrent'eva 13/3, 630090 Novosibirsk, Russia

Received 25 June 2003; revision received 9 January 2004
Kvantovaya Elektronika **34** (4) 341 – 347 (2004)
Translated by M.N. Sapozhnikov

that, for the detuning $\delta = 0$, the residual magnetic field should be lower than 10^{-2} G.

2. Methods for detecting a new friction force

The choice of a particular experimental scheme is determined by a number of physical restrictions and technical possibilities. There exist three methods to detect the force predicted in Ref. [6]: (i) the cooling of atoms directly under the above-described conditions in the one-dimensional geometry in the absence of a quadrupole magnetic field (without a conservative force); (ii) the initial accumulation of cold atoms in a purely viscous three-dimensional trap [9, 10] (i.e., in the absence of a magnetic field, but with the red shift of the laser frequency) followed by the switching of frequency, polarisation, and intensity; and (iii) the accumulation of many cooled atoms in a substantially smaller volume of a MOT under optimal conditions (the red frequency shift of the order of a few γ, circular [11] or linear [12] polarisation, inhomogeneous magnetic field, and comparatively high intensity) followed by fast changes in the frequency, polarisation and intensity and by switching off the magnetic field.

For the zero detuning of the cooling laser frequency from the atomic resonance, the known Doppler mechanisms of friction have the zero efficiency and maximum diffusion. As a result, fast atoms are not virtually cooled and their concentration in the molasses will be very low. Under these conditions, it is rather difficult to observe the dissipation mechanism for slow atoms predicted in Ref. [6]. Therefore, we do not consider here the first method.

The two other methods require the frequency and polarisation switching (in the third method, a magnetic field should be also switched off) and the switching time should be much shorter than the fly-off time of cold atoms. The study of the dependence of the number of atoms captured in a MOT on the degree of ellipticity of polarisation of laser fields performed in this paper showed that atoms are efficiently accumulated at elliptic polarisations as well, so that no polarisation switching is required, which substantially simplifies the experiment.

A key moment is the possibility of stabilisation with an accuracy to a few fractions of γ and fast switching of the laser frequency within a few γ in the vicinity of the cooling transition frequency. In this case, the laser linewidth should be much narrower than γ and, therefore, the broadening of the spectrum due to modulation required for production of the error signal is inadmissible (the frequency of the reference resonance should be modulated rather than the laser frequency). Note also a number of additional requirements. When a conservative force is switched off, the scattering of atoms strongly depends on the unbalance of intensities of counterpropagating fields, when their frequency lies in the region of an exact resonance. For this reason, we did not use retroreflective mirrors and all the six beams were formed separately. The maximum total intensity of beams inside the trap should be of the order of the saturation intensity (~ 1.6 mW cm^{-2} for the D_2 line of ^{85}Rb) and should be decreased in a controllable way down to the intensity at which sub-Doppler cooling occurs. To accumulate many atoms efficiently, laser beams should have homogeneous profiles and large diameters [13].

The possibility of using the three-dimensional configuration of cooling beams instead of the one-dimensional configuration considered in Ref. [6] is based on the following considerations. First, the existence of the anomalous component of the friction force, which is nonzero on average in the space, follows from the symmetry relations that take place in the three-dimensional case as well. Second, because of phase fluctuations of the interfering beams in the molasses, the actions of crossed laser beams on atoms become mutually independent.

3. Experimental technique

We used a diode laser with an anti-reflection coating and an external diffraction grating in the Littmann mounting to cool atoms.

The stabilisation scheme is based on the Zeeman shift of levels in a homogeneous magnetic field. A sub-Doppler resonance is produced as the difference between the intensities of two probe beams of a small diameter transmitted through an atomic cell. A saturating beam of a large diameter propagates towards one of the probe beams. All the three beams have the same circular polarisation (Fig. 1). This method provides the compensation for the Doppler broadened response of the system to a change in the magnetic field, which is independent of the saturating field. In particular, the modulation of the width and amplitude of the Doppler profile of the line caused by a change in the distance between magnetic sublevels is suppressed in the difference signal. The scheme of the resonance formation, in which atoms are accumulated in one magnetic sublevel, allows the variation in the resonance frequency by a magnetic field without the resonance broadening. The stabilisation scheme is close to that considered in Refs [14, 15] but it uses, unlike Refs [14, 15], a nonlinear

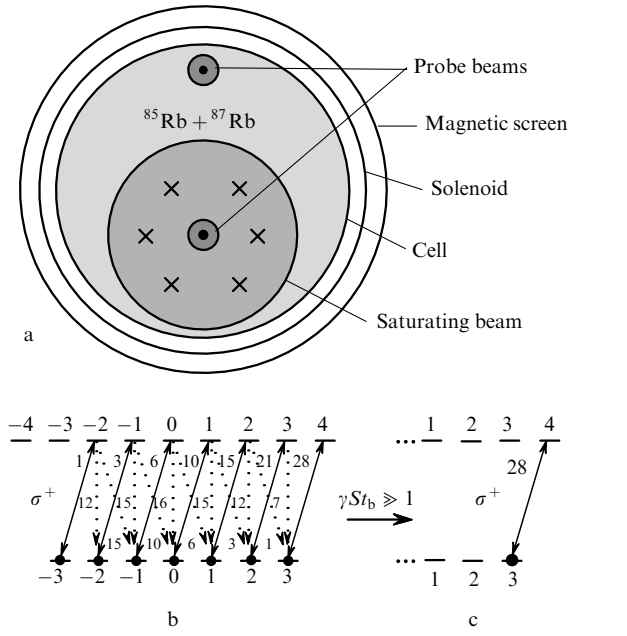

Figure 1. Mutual arrangement of the saturating and probe beams in an atomic cell (a); the relative transition probabilities in the system of magnetic sublevels of the ground state of rubidium in a circularly polarised field resonant with the cyclic $5S_{1/2}(F = 3) - 5P_{3/2}(F' = 4)$ transition (^{85}Rb) (b); the transfer of atoms on the extreme sublevel due to repeated absorption-emission cycles (c). The solid and dotted arrows are stimulated and spontaneous transitions, respectively.

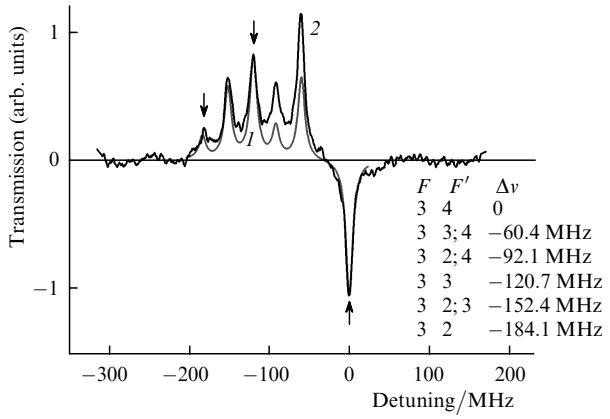

Figure 2. Comparison of the theoretical (*1*) and experimental (*2*) saturated absorption spectra at the D_2 line of ^{85}Rb in the zero magnetic field. Three of the six resonances indicated by arrows correspond to the hyperfine-structure transitions $F = 3 - F' = 2, 3, 4$. The rest of the transitions are crossovers. For all the resonances, except $F = 3 - F' = 4$ (zero detuning), the redistribution of atoms among the ground-state sublevels and the transition to the excited state reduce absorption.

peak rather than a hole in absorption. Upon frequency stabilisation, a transmission minimum at the line centre is useful for minimisation of shot noise in the detection scheme. The sub-Doppler absorption peak is separated from the rest of resonances in the D_2 line (Fig. 2).

Figure 3 shows the stabilisation scheme including the three-beam scheme to shape the reference signal in one cell and the two-beam scheme to observe the reference polarisation resonance in the second cell. The rotation of the polarisation plane of probe beams in two successive quarter-wave plates provides the separation of the probe and saturating beams with the help of a polarisation beamsplitter cube. A combined use of a screen at the central part of the saturating beam and a blocking aperture not only

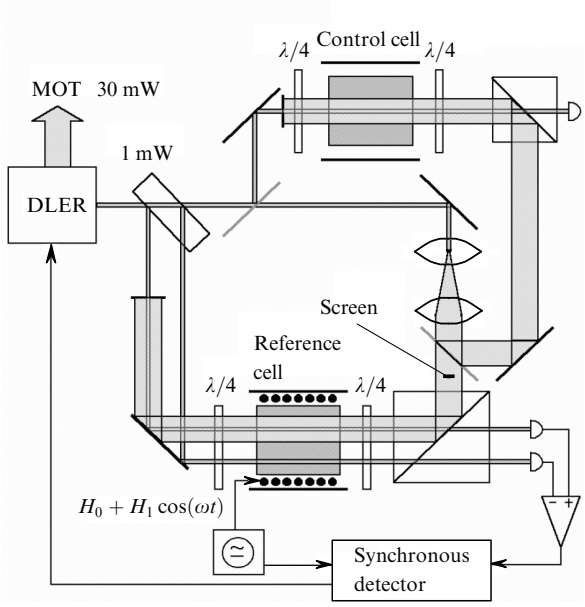

Figure 3. Scheme for frequency stabilisation of an diode laser with an external resonator (DLER) by the sub-Doppler absorption resonance in an atomic cell.

eliminates a competing mechanism of two-level nonlinearity (see section 5) but also suppresses a parasitic optical feedback in the laser.

The shift of the resonance at the extreme magnetic sublevel is proportional to a constant magnetic field of a solenoid in which the reference cell is placed. A modulating signal at the frequency 15 kHz, which produces the error signal, is fed to this solenoid. Therefore, the laser frequency is not modulated and the laser line is not broadened. The frequency shift of the reference resonance in the magnetic field equal to 1.4 MHz G^{-1} coincides with its theoretical value. The instability of the current source of a coil is 10 μA, corresponding to the instability of the magnetic field in the cell equal to 150 μG. The background longitudinal magnetic field in the reference cell is screened down to ~ 2 mG.

The error signal of the AFC system was fed, after synchronous detection, integration, and amplification (Fig. 4), to a piezoelectric element controlling the resonator length. The feedback band of the system at the −3 dB level was 2 kHz. The frequency detuning in the capture regime was determined by using the nonlinear absorption resonance in the control atomic cell formed by two counterpropagating beams with the same circular polarisation. The beam diameters and intensities were as those in the reference cell (Fig. 3). The background longitudinal magnetic field in the control cell was screened down to ~ 20 mG.

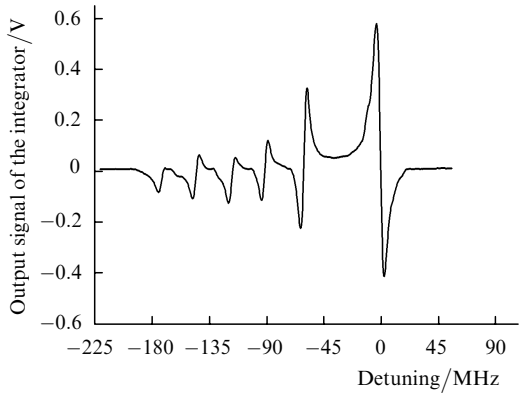

Figure 4. Discrimination curve for resonances at the $5S_{1/2}(F = 3)$–$5P_{3/2}(F' = 2, 3, 4)$ transition obtained by modulating the longitudinal magnetic field in the reference cell with ^{85}Rb and detecting synchronously the difference absorption signal of two probe beams. The saturating beam intensity is 0.1 mW cm^{-2} and the recording time is 120 s.

Figure 5a shows the transient characteristic of the stabilisation system observed upon a fast change in the current in the solenoid of the reference cell. The time constant of the integrator in the stabilisation system was 1 ms and the duration of the aperiodic transfer process was a few milliseconds. Figure 5b shows the scheme of frequency calibration using the resonance slope in the control cell.

The width of the noise path during the frequency tuning to the resonance slope in the reference cell (laser frequency fluctuations) was 300 kHz in the 15-kHz bandwidth of the detector. In the white noise approximation, this corresponds to 2.5 kHz in the 1-Hz bandwidth. Therefore, the instability of the laser frequency was 7×10^{-12} Hz$^{1/2}$. The study of the dissipative light pressure force of a new type assumes laser frequency stabilisation in the region of detunings close to zero. In the stabilisation system described above, this

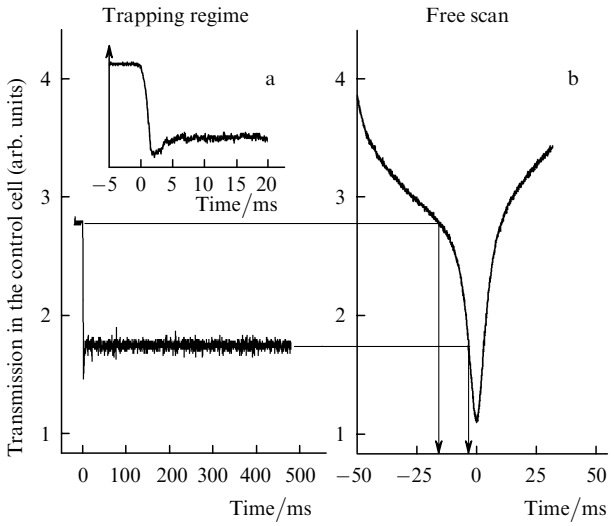

Figure 5. Transmission in the reference cell during a 'step' variation of the magnetic field in the reference cell in the regimes of stabilisation (a) and free scan (b) of the laser. Figure 5b shows the method for determining the frequency detuning. The inset at the left top shows the initial stage of frequency switching.

corresponds to the absence of a magnetic field in the reference cell. In the absence of an appreciable longitudinal component of the magnetic field, the transverse background component can change the selection rules in the interaction with a circularly polarised field, therefore, the laboratory field should be screened. The residual magnetic field splits Zeeman sublevels, thereby restricting the minimum intensity of a saturating field, i.e., the rate of optical pumping in the ground state should exceed this splitting.

A slight deviation of polarisation of a light field from purely circular polarisation, i.e., the presence of a linearly polarised component in it, in the region of a zero magnetic field leads to formation of coherent superposition states with increased or decreased absorption. The presence of such states violates the operation of the stabilisation system. These effects are known in the literature as electromagnetically induced absorption (EIA) [16] and electromagnetically induced transparency (EIT) [17]. In the system for frequency stabilisation and tuning based on the Zeeman effect, EIA leads to the distortion and even discontinuity in a linear dependence of the laser frequency on the longitudinal magnetic field (with increasing the deviation of polarisation from the circular one and in the presence of the transverse component of the field).

On the other hand, the polarisation state can be accurately adjusted and the transverse component of the field can be suppressed by the minimum of the EIA resonance. In addition, the resonance allows us to calibrate the zero of the longitudinal component of the magnetic field. In our opinion, this resonance was the reason for a 'puzzling' violation of the linearity of frequency tuning in the zero magnetic field, which was pointed out in Ref. [4]. Figure 6 illustrates the dependence of a saturated absorption signal in the reference cell on the magnetic field near the line centre. The narrow photoinduced absorption resonance at the line centre at the cyclic transition has the width of ~ 150 kHz and appears due to a slight deviation of polarisation of the saturating beam from a purely circular polarisation.

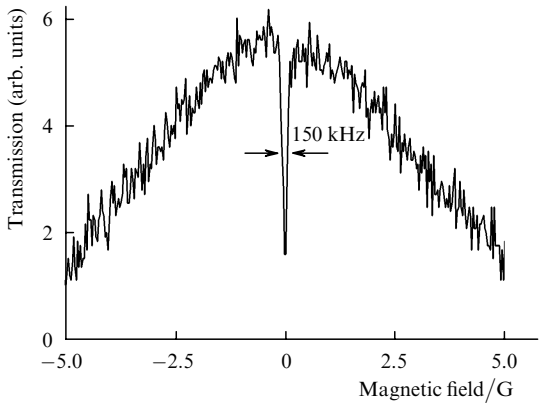

Figure 6. Typical shape of the photoinduced absorption resonance in the reference cell in the case of incomplete elimination of the linearly polarised component in a saturating field.

4. Magnetooptical trap

The main parameters of the MOT are as follows. Pressure in a metal chamber with AR windows, which is connected to a magneto-discharge pump, is kept at the 10^{-8} Torr level. The background concentration of Rb atoms supplied from a glass outlet of the chamber, whose temperature is controlled, and the residual pressure of other gases determined the accumulation time for atoms in the trap (0.7 – 1 s). Six beams of a cooling laser of intensity up to 3 mW cm^{-2} and diameter 10 mm are incident into the chamber each through its own window. In all the beams, quarter-wave plates in rotatable mounts are placed, which specify the polarisation ellipse of cooling beams. Four beams from a pump laser with the total power of 1 – 2 mW are incident into the chamber along the vertical and one of the horizontal directions. The magnetic field gradient in the middle of the chamber (where the magnetic field is zero) can achieve the value of 6 G cm^{-1}, which is restricted by the heating of paired coils, the ratio of gradients along and across of the axis of these coils being 1.9 : 1. In the case of optimal parameters, up to 1.5×10^7 atoms with the characteristic size of the cloud equal to 0.4 mm and temperature from 20 to 50 μK can be accumulated in the trap. The fluorescence dynamics of trapped atoms is observed by means of a lens system imaging an ensemble of cooled atoms and a photomultiplier placed behind the aperture. The ensemble image is also controlled with a TV system consisting of a CCD camera and a monitor.

Figure 7a shows the fluorescence signal of cold atoms in the MOT, and Fig. 7b demonstrates the transmission signals observed in the control cell when the cooling laser frequency was slowly tuned near the transition frequency. The frequency of the stabilised laser was decreased linearly near the cooling transition during the first 100 s, then it was increased during 50 s, and then was fixed at the −10-MHz detuning. A small drift velocity of the signal level at the slope of a frequency discriminator (the lower curve in Fig. 7b) provided a long-term stable operation of the stabilisation system of the cooling laser. Fluorescence collected from the trap (the upper curve in Fig. 7b) has a local minimum near the exact resonance, which is caused by the transition saturation in background Rb vapours in counterpropagating fields.

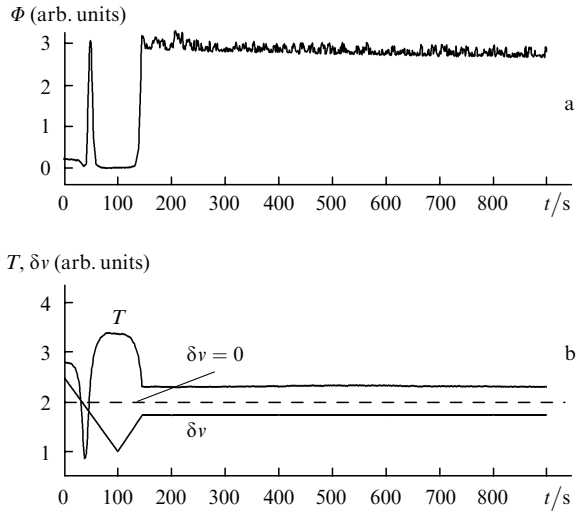

Figure 7. Time dependences of the fluorescence intensity Φ of an ensemble of cold atoms in a trap (a) and transmission T in the control cell and the laser frequency detuning $\delta\nu$ (b). The recording time is 15 min.

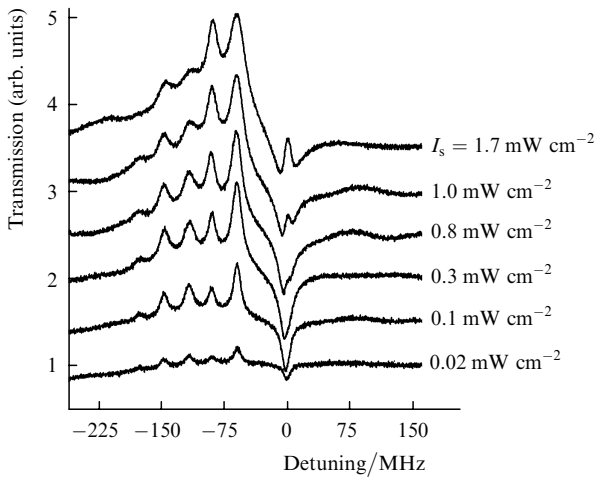

Figure 8. Transmission spectra for the D_2 line of ^{85}Rb for different intensities of the saturating beam in a zero magnetic field.

5. Contrast of the polarisation resonance

In the scheme of counterpropagating beams (Fig. 1a), two nonlinear mechanisms act simultaneously: a decrease in absorption due to transfer of a part of atoms to the excited state ($5P_{3/2}$, $F' = 4$) and an increase in absorption due to optical pumping to the extreme magnetic sublevel of the ground state ($5S_{1/2}$, $F = 3$, $m = 3$) (Figs 1b, c). We will call them the two-level and polarisation saturation mechanisms, respectively.

The relaxation time of polarisation in the ground state is determined by the time t_f of flight of an atom through a light beam. It is much longer than the excited-state lifetime γ^{-1}. To pump atoms efficiently to the extreme magnetic sublevel, a great number of absorption–emission events are required, which are described by the dimensionless parameter $\gamma S t_f$ of polarisation saturation in the ground state, where S is the saturation parameter in a two-level system. An increase in absorption upon pumping atoms to the extreme magnetic sublevel is caused by the fact that the absorption probability in the cyclic $F \to F+1$ transition from the extreme magnetic sublevel in a circularly polarised field is higher than on average over the multiplet (Fig. 1b). Because of the competition between the two above mechanisms, the shape and sign of the nonlinear resonance are determined by the intensity and diameter of the saturating beam. When the beam diameter is small and its intensity is high, a hole dominates in the absorption signal. As the beam diameter increases and its intensity decreases, the hole is replaced by a peak. In the case of intermediate values of these parameters, a broad polarisation peak contains a narrow two-level hole (see Fig. 8 and also Ref. [18]). The different width of the peaks is caused by the difference of the saturation parameters S and $\gamma S t_f$. Note that both nonlinear mechanisms reduce absorption at other transitions of the D_2 line.

Let us estimate optimal conditions for the observation of polarisation resonance. The maximum contrast of nonlinear absorption with respect to linear absorption is realised when total absorption in an optically thin cell is weak. In the case of an infinitely broad low-intensity saturating beam ($S \ll 1$ but $\gamma S t_f \gg 1$), optical pumping leads to an ultimate polarisation of the ground state, which is homogeneous within the volume where probe radiation propagates. Let α_{lin} and α_{nl} be the absorption coefficients at the line centre in the absence and presence of the saturating field, respectively. The contrast $c_{nl} = (\alpha_{nl} - \alpha_{lin})/\alpha_{lin}$ of the nonlinear absorption peak can in principle exceed unity. In the limit $\gamma S t_f \gg 1$, we have [19]

$$\alpha_{nl}^{max} \propto \left(C_{F,F,1,1}^{F+1,F+1}\right)^2 = 1,$$

$$\alpha_{lin}^{max} \propto \frac{1}{2F+1}\sum_m \left(C_{F,m,1,1}^{F+1,m+1}\right)^2 = \frac{2F+3}{3(2F+1)}, \qquad (1)$$

$$c_{nl}^{max} = \frac{4F}{2F+3},$$

where F is the total angular momentum of the ground state and $C_{F,F,1,1}^{F+1,F+1}$ and $C_{F,m,1,1}^{F+1,m+1}$ are the Clebsch–Gordon coefficients. For rubidium isotopes, the maximum contrasts are $c_{nl}^{max}(^{87}\mathrm{Rb}) = 8/7$ (114 %) and $c_{nl}^{max}(^{85}\mathrm{Rb}) = 4/3$ (133 %). Figure 9 shows the calculated dependences of the contrast of the nonlinear resonance on the intensity and flight time in an optically thin cell in the case of simultaneous action of the two above-mentioned mechanisms (the lower curves in each pair of curves). However, if linear absorption is too small, the linear component is also small. When absorption increases (due to an increase in the concentration of atoms or the cell length), the intensity of the saturating field and polarisation of the medium become spatially inhomogeneous and the contrast of the nonlinear resonance decreases although the number of probe photons absorbed at the line centre increases.

In this case, the coefficients α_{lin} and α_{nl} describe local absorption, and we will denote the fraction of the absorbed total power by A_{lin} and A_{nl} for linear and nonlinear cases, respectively. In the case of strong linear absorption ($A_{lin} \sim$ 100 %), the nonlinear addition is negligibly small. We can roughly estimate the total absorption in the cell, in which the nonlinear component is maximal, assuming that absorption is homogeneous in the central region of the saturating beam over the entire length L of the cell, the ground-state

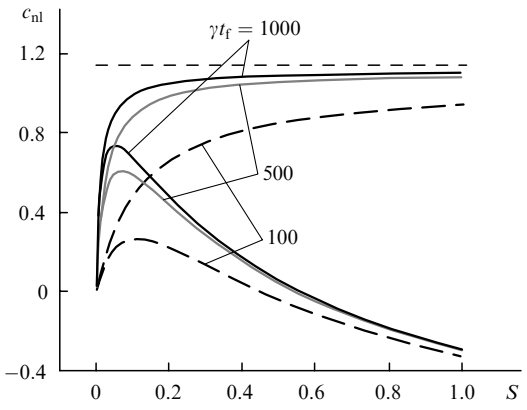

Figure 9. Theoretical dependences of the nonlinear contrast $c_{nl} = (\alpha_{nl} - \alpha_{lin})/\alpha_{nl}$ at the cyclic transitions from the $F = 2$ level of the ground state of ^{87}Rb on the saturation parameter S. The upper curve in each pair of curves for the same value of γt_b corresponds to the scheme with the screening of the central part of the saturating beam. The horizontal dashed curve is the ultimate contrast (114 %) discussed in the text.

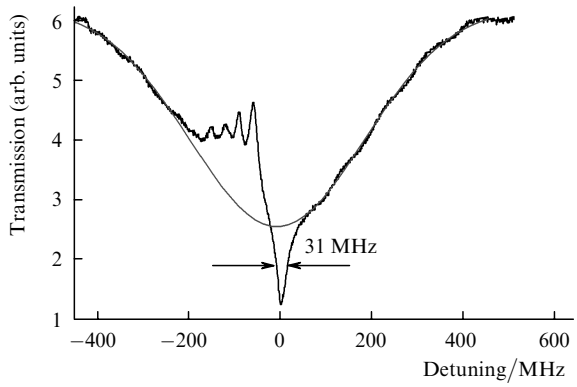

Figure 10. Nonlinear resonance at the $5S_{1/2}(F = 3) - 5P_{3/2}$ $(F' = 4)$ transition in ^{85}Rb with the 38 % contrast obtained for the saturating beam intensity $I_s = 1.7$ mW cm^{-2} and diameter 14 mm. At the central part of the beam, a screen of diameter 2.5 mm was placed, in whose shadow the probe beam of diameter 2 mm with the intensity of 0.1 mW cm^{-2} propagated. The smooth curve is the Gaussian approximation of the linear absorption line, which was plotted by the absorption data at the line wings.

polarisation has the ultimate value and relations (1) are valid. Linear absorption in a homogeneous medium is $A_{lin} = 1 - t$, where $t = \exp(-\alpha_{lin} L)$ is the transmission in the cell, and a change in transmission at the line centre caused by the saturating field is

$$A_{nl} - A_{lin} = t - t^{\beta}, \quad \beta = \frac{\alpha_{nl}^{max}}{\alpha_{lin}^{max}}. \tag{2}$$

The nonlinear addition (2) is maximal for $t = \beta^{-1/(\beta-1)} \approx 50\,\%$:

$$(A_{nl} - A_{lin})_{max} = \beta^{-\beta/(\beta-1)}(\beta - 1), \tag{3}$$

which comprises 30 % of the radiation power incident on the cell and 60 % of linear absorption. Therefore, the contrast of nonlinear resonance in a 'thick' cell under optimal observation conditions is approximately half the ultimate contrast (1). The exact values of the contrast for isotopes are slightly different, however, there is no point in refining estimates within the framework of our model.

Figure 2 shows the experimental and theoretical [20] signals of saturated absorption for identically oriented circular polarisations of the probe and saturating beams at the D_2 line of ^{85}Rb. The expression obtained in Ref. [20] describes the absorption probability at all hyperfine-structure transitions for $\gamma t_f \gg 1$ and $\gamma S t_f < 1$ and takes into account scalar, magnetic dipole, and quadrupole scattering, which are of the same order of magnitude. Good agreement is observed between the theory and experiment for intrinsic resonances (indicated by arrows).

We proposed in this paper the method for eliminating a competition between two nonlinearity mechanisms, which uses a partial screening of the saturating in the region of propagation of the probe beam of a lower diameter. Figure 10 shows the example of nonlinear resonance absorption with the nonlinear contrast $c_{nl} = 38\,\%$ ($t = 5\,\%$) for the saturating beam intensity close to the intensity of two-level saturation. The central part of the beam was screened. The dependence of the nonlinear contrast on the intensity in this situation is shown in Fig. 9 (the upper curves in each pair of curves). As $\gamma S t_f$ increases, the contrast of the polarisation resonance tends to the maximum value (3), however, the width of the resonance also begins to increase.

6. Conclusions

We have developed the system for frequency control and stabilisation in a diode laser near the frequency of a cyclic cooling transition in Rb atoms. The frequency tuning range is $+40 \ldots -150$ MHz. The short-term frequency stability, estimated from the transmission signal at the slope of the independent control resonance neglecting its own fluctuations, is 2.5 kHz in the 1-Hz band. We have proposed the method for enhancing the contrast of a sub-Doppler resonance by screening partially the saturating beam. A high contrast (up to 50%) was obtained for the sub-Doppler resonance at the cyclic transition. We explained the anomalous behaviour of the stabilisation system in the zero magnetic field in the reference cell by taking into account EIA and EIT phenomena and also proposed the method for eliminating this effect, which violates the frequency stabilisation regime. Our calculation confirmed the presence of the anomalous friction force in elliptical light fields in the case of the zero detuning and the ground-state angular momentum $F > 1/2$. We also calculated the dependences of the contrast of the polarisation resonance at the cyclic transition on the intensity and time of the interaction.

Acknowledgements. The authors thank V.A. Sautenkov, E.R. Eliel, and J.P. Woerdman for placing the vacuum part of the MOT at our disposal, V.P. Yakovlev, V.K. Egorov, and A.A. Tumaikin for useful advises and discussions, and S.A. Zibrov and E.S. Knyazchan for their help in experiments. This work was supported by the ISTC (Grant No. 2651p).

References

1. Ikegami T., Sudo S., Sakai Y. *Frequency Stabilization of Semiconductor Laser Diodes* (Boston, London: Artech House, 1995).

2. Kitching J., Knappe S., Vukicevic N., Hollberg L., Wynands R., Weidmann W. *IEEE Trans. Instr. Meas.*, **49**, 1313 (2000).
3. Oates C.W., Hollberg L., et al. *Opt. Lett.*, **25**, 1603 (2000); Celikov A., Riehle F., Velichansky V.L., Helmcke J. *Opt. Commun.*, **107**, 54 (1994).
4. Balykin V.I., Minogin V.G., Letokhov V.S. *Rep. Prog. Phys.*, **63**, 1429 (2000).
5. Adams C.S., Riis E. *Prog. Quantum Electron.*, **21**, 1 (1997).
6. Prudnikov O.N., Taichenachev A.V., Tumaikin A.M., Yudin V.I. *Pis'ma Zh. Eksp. Teor. Fiz.*, **70**, 439 (1999).
7. Dalibard J., Cohen-Tannoudji C. *J. Opt. Soc. Am. B*, **6**, 2023 (1989).
8. Prudnikov O.N., Taichenachev A.V., Tumaikin A.M., Yudin V.I. *Tech. Dig. IQEC/LAT* (Moscow, 2002).
9. Chu S., Hollberg L., Bjorkholm J.E., Cable A., Ashkin A. *Phys. Rev. Lett.*, **55**, 48 (1985).
10. Hope A., Haubrich D., Schadwinkel H., Strauch F., Meshede D. *Europhys. Lett.*, **28**, 7 (1994).
11. Lindquist K., Stephens M., Wieman C. *Phys. Rev. A*, **46**, 4082 (1992).
12. Emile O., Bardou F., Salomon C., Laurent Ph., Nadir A., Clairon A. *Europhys. Lett.*, **20**, 687 (1992).
13. Gibble K.E., Kasapi S., Chu S. *Opt. Lett.*, **17** (7), 526 (1992).
14. Dinnen T.P., Wallace C.D., Gould P.L. *Opt. Commun.*, **92**, 277 (1992).
15. Ikegami T., Ohshima S., Ohtsu M. *Jpn. J. Appl. Phys.*, **28** (10), 1839 (1989).
16. Akulshin A.M., Barreiro S., Lezama A. *Phys. Rev. A*, **57** (4), 2996 (1998); Lezama A., Barreiro S., Akulshin A.M. *Phys. Rev. A*, **59** (6), 4732 (1999).
17. Arimondo E., in *Progress in Optics*. Ed. by E. Wolf (Amsterdam: Elsevier, 1996) Vol. XXXV, pt. V, pp 256 – 354.
18. Gamidov R., Taskin I., Sautenkov V. *Proc. Fifth Symposium on Frequency Standards and Metrology* (Massachusetts: Woods Hole, 1995) pp 445 – 449.
19. Private communication.
20. Akul'shin A.M., Velichansky V.L., Krasheninnikov M.V., Sautenkov V.A., Smirnov V.S., Tumaikin A.M., Yudin V.I. *Zh. Eksp. Teor. Fiz.*, **96**, 107 (1989).